FABRICATION AND CHARACTERIZATION OF PLASTIC SCINTILLATORS AND MEASUREMENTS OF MUON FLUX AT EARTH

Submitted by:

Vishnuprasad P.R

Sree Narayana College,

Chengannur,

Kerala University.

Under the guidance of:

Dr. Prashant Shukla

Nuclear Physics Division,

Bhabha Atomic Research Centre,

Mumbai 40085, India.

ACKNOWLEDGEMENT

I am sincerely thankful to Dr. Prashant Shukla (Scientific Officer-H) for his guidance to do my project.

Also, I would like to express the foremost gratitude to Mr. Hariom (Research Scholar, INO) for his support to complete the project. His valuable suggestions helped me a lot.

ABSTRACT

Plastic scintillators are widely used in high energy experiments to detect a variety of particles. We used a general purpose plastic scintillator of dimension 100 cm $\times$ 10 cm $\times$ 2.5 cm. Light guides are used to couple photomultiplier tubes on both the ends of the bar. Tyvek and tedler papers are used for light reflection and light tightening. Three such detectors are made and their characteristics such as rise time and efficiency are measured. Two configurations made by scintillators are used to measure the muon flux.

CONTENTS

CHAPTER ONE

INTRODUCTION

Scintillator exhibits scintillation, the property of luminescence, when excited by ionizing radiation. Luminescent materials, when struck by an incoming particle, absorb its energy and emit light. The first device which used as a scintillator was built in 1903 by Sir William Crookes and used a ZnS screen. The scintillations produced by the screen were visible to the naked eye if viewed by a microscope in a darkened room, the device was known as a spinthariscope. Curran and Baker in 1944 replaced the naked eye measurement with the newly developed PMT. This was the birth of the modern scintillation detector. Scientists at Lawrence Livermore National Laboratory have developed a plastic scintillator that can detect neutrons, something previously thought impossible. They found that plastic scintillators have a roughly 20 percent finer resolution for neutron-gamma ray discrimination than liquid scintillators. Plastic scintillator detects neutrons could be far cheaper and more flexible than traditional detectors. We selected plastic scintillator to detect muon particles. Muons can be used to study about properties of new discovered substances behaviour at the very small scale. Muons are used for studying magnetism, superconductivity, diffusion and charge transport. Muons can also be thought of as light protons and studies of their behaviour inside substances can shed light on hydrogen behaviour in technologically relevant semiconductors. In this experiment, we fabricated three plastic scintillator detectors to measure the atmospheric muon flux. Also, we measured the efficiency of the detectors and plotted the efficiency curve. We used liquid scintillators for triggering. This project also mentioned about rise time of plastic scintillator and the comparison with liquid scintillator.

REVIEW OF LITERATURE

R.A. MEWALD, 1996 : His article gives general introduction to the field of cosmic rays which was published in the Macmillan Encyclopedia of Physics in 1996. It describes the fundamental idea about discovery and early researches on cosmic rays. It gives the ideas of cosmic ray composition and it's effect in solar system.

Steve Kliewer, Endeavour Academy : He published an article which gives ideas about origin of different particles from the cosmic rays. It provides fundamentals of different particles like rest mass, decay mode, mean life etc. The concepts of muon particles gives the ideas of it's basic characteristics.

Glenn F Knoll, 1999 : This is the basic source of any research scholor who is working in detectors. It gives ideas of many detectors, it's working and characteristics. This book provided to me the ideas of scintillators, photomultiplier tubes, voltage divider and coaxial cable etc.

CHAPTER TWO

THEORY

2.1 Cosmic Rays

Victor Hess discovered cosmic rays in 1912 in a series of high altitude balloon flights. In that period, physicists knew of an anomalous radiation that would discharge electroscopes, early instruments used to measure electric charge. The source of this radiation was unknown and scientists speculated whether the source of the radiation was terrestrial or extra terrestrial in origin. Taking electroscopes on manned balloon flights in excess of 5 km in altitude, Hess found that the rate of these discharges increased with altitude, showing that the radiation was coming from space. The actual name "cosmic ray" was coined ten years later by Robert Andrews Millikan in 1925 [1].

Cosmic rays are stable charged particles that have been accelerated to enormous energies by astrophysical sources somewhere in universe. They are charged because accelerating mechanism is probably electromagnetic and because their charge is somewhat interacts with matter and produces effects that we can easily see here on earth. They have a range of energies 10^9 eV up to 10^{20} eV. The best we can acheive in the latest accelerators here on earth is about 7 TeV. Cosmic rays are classified into 2 types. They are primary cosmic rays and secondary cosmic rays. Technically, "primary" cosmic rays are those particles accelerated at astrophysical sources and "secondaries" are those particles produced in interaction of the primaries with interstellar gas. 95% of all cosmic rays are protons, 4% are helium nuclei and 1% balance is made up of nuclei from other stellar-synthesized elements. Their flight paths are uniform across the galaxy, they strike earth at random orientations. A major factor affecting the path of cosmic rays is

that they are charged and therefore swerved by magnetic field. Magnetic fields exist throughout space.

The Galaxy, Sun and the Earth each strongly affect the particle's path. The more energy a particle has, greater the radius of curvature. Particles with energies less than 10^{15} eV have paths that are so curved that they are probably trapped within our galaxy and wander throughout. The Earth's field also affects direction and tends to exclude lower energy particles.

The particles have greater difficulty penetrating the Earth's field near the equator than they do near the magnetic poles. Cosmic ray muons are created when cosmic rays enter earth's atmosphere where they eventually collide with an air molecule and initiate a hadronic shower i.e. a cascade of particles (mostly pions) that may undergo further nuclear reactions. Cosmic muons are leptons like electrons. But, it is very massive than electron and has a very short mean lifetime. In fact, its life is so short that it shouldn't be able to make it to the surface. Yet, it is observed to be the most common high energy particle to be seen here at the ground. This is an oppurtunity to see a real life example of relativistic time dilation.

The primary cosmic rays collide with the nuclei of air molecules and produce a shower of particles that include protons, neutrons, pions (both charged and neutral), kaons, photons, electrons and positrons. These secondary particles then undergo electromagnetic and nuclear interactions to produce yet additional particles in a cascade process. Figure 1 indicates the general idea. Of particular interest is the fate of the charged pions produced in the cascade. Some of these will interact via the strong force with air molecule nuclei but others will spontaneously decay (indicated by the arrow) via the weak force into a muon plus a neutrino or antineutrino. The decay is shown below

$$\pi^+ \rightarrow \mu^+ + \nu_\mu$$

$$\pi^- \rightarrow \mu^- + \bar{\nu_\mu}$$

The muon does not interact with matter via the strong force but only through the weak and electromagnetic forces. It travels a relatively long distance while losing its kinetic energy and decays by the weak force into an electron plus a neutrino and anti-neutrino. At sea level, about 70% of secondary cosmic rays are mesons, 29% are electron-positron pairs while 1% are heavy particles.

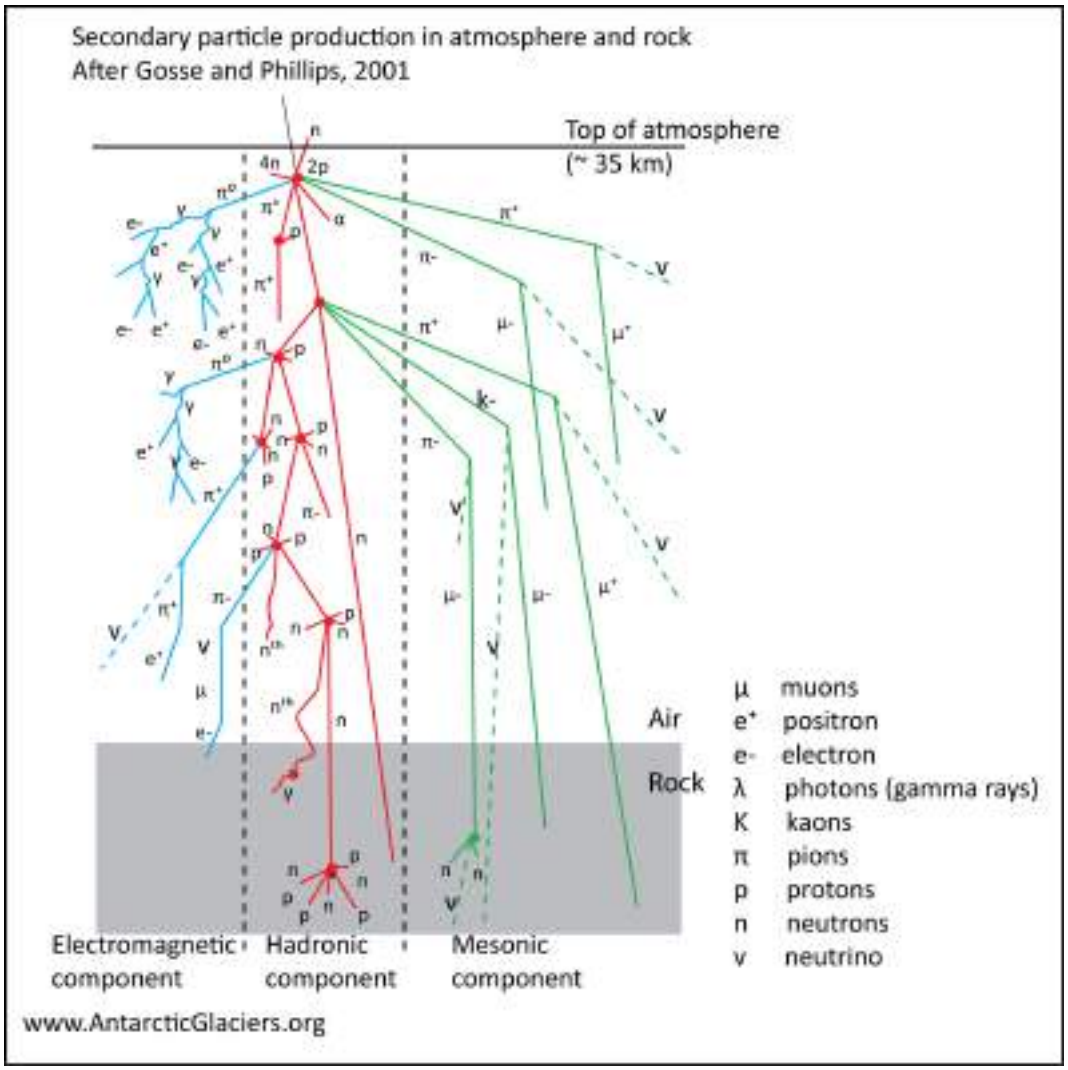

Figure 1: A schematic representation of cosmic ray shower

Atmospheric interactions

Primary cosmic rays wandering through interstellar space which have density about $10^{-23} g/cm^3$), suddenly encounters our atmosphere where the density rapidly rises 20 orders of magnitude to 10^{-3} g/cm^3 at sea level, it very likely collide with particles of air.

These interactions produce three kinds of pions (positive, negative and neutral) and two kinds of kaons (positive and negative). Pions and kaons are mesons (particles made up of a quark-antiquark combination) and have extremely short life times. The charged pions with mean life times of 26 nanoseconds and kaons with lives of 12 nanoseconds, which decay into muons which have lives 1000 times longer (2.2 microseconds). The neutral pions decay almost immediately (10^{-16}s) into gamma rays. The muons can decay into electrons or positrons but, their lifetime is long enough that they usually make it all the way to the ground.

The high-energy gamma rays start an electromagnetic cascade of electrons and positrons. Pair production (electron/positron pair) occurs when gamma rays encounter air nuclei. Bremsstrahlung ("breaking radiation") occurs when resultant electrons pass near air nuclei producing more gamma rays, which in turn produce more electrons.

At sea level, for every 10000 muons, there will still be roughly: 200 primaries (protons and occasional neutrons), 20 high energy electrons (E $>$ 1 GeV) and 4 pions. But, there may be up to 100000 low energy electrons created by cascade. These particles are absorbed quickly but, if the shower is energetic enough or the shower started low enough, they may still be the most prevalent particles at sea level. However, because of their lack of penetrating power, plastic scintillators we are using, won't detect them anyway. The properties of different particles are mentioned in the table 1.

Table 1: Properties of different particles [2]

Particle	Rest Mass Energy	Mean Life	Decay Mode	Branching Ratio
p	940 MeV	$>10^{25}$ years	-	-
n	940 MeV	887s	p $e^{-}\nu_e$	1
π^+	140 MeV	26 x 10^{-9}s	$\mu^+\nu_\mu$	0.99
π^0	130 MeV	8 x 10^{-17}s	2γ	0.99
K^+	500 MeV	12 x 10^{-9}s	$\mu^+\nu_\mu$	0.63
μ^+	105 MeV	2.2 x 10^{-6}s	$e^+\nu_e\nu_\mu$	0.99
ν_μ	<0.3 MeV	<50 days	?	-
e^-	0.51 MeV	$>10^{23}$years	-	-
ν_e	$\sim$5eV	$\sim$25 min	?	-

2.2 Muons

Muons are exactly the same as an electron except heavier. The mass of a muon is 207 times the mass of an electron. So, muon has properties similar like electron. There is a good reason why the muon is such an unfamiliar particle: muons are radioactive and they decay with a half-life of 1.52 microseconds. That is 1.52 x10^{-6} seconds or 1.52 millionths of a second. Not $5,700$ years, like C^{14}, but 1.52 millionths of a second. The muon was discovered in 1936 by Carl Anderson, a physicist at Caltech. By the way, shortly before this, in 1932-33, Anderson had discovered another unusual particle called the positron. The positron, which is exactly like an electron but with positive instead of negative electric charge, is sometimes called an antielectron and was the first discovered member of a whole category of particles known as antimatter. Carl Anderson won the Nobel Prize in 1936 for the discovery of antimatter.

Muons are the most numerous energetic charged particles at the sea level. A charged particle cannot avoid losing energy by ionisation. As it passes through matter the charged particle interacts with electric fields and typically knocks loose some of the loosely bound outer electrons. A muon interacts very little with matter except by ionisation. Because of this, muons can travel large distance and commonly reach the ground. However, they lose energy proportional to the amount of matter they pass. This is proportional to the density (g/cm^3) times the path length (cm). This "interaction length" has unit of gram per square centimeter.

Muons lose energy at a fairly constant rate of about 2 MeV per g/cm^2. Since, the vertical depth of the atmosphere is about 1000 g/cm^2, muons will lose 2 GeV to ionisation before reaching the ground. The mean energy of muons at sea level is still 4 GeV. Therefore, the mean energy at the creation is probably about 6 GeV. The atmosphere is so tenuous at higher altitudes that even at 15000 m it is still only 175 g/cm^2 deep. Typically, it is about here that most muons are generated. Muons arrive at sea level with an average flux of about 1 muon per square centimeter per minute. This is about half of the typical total natural radiation background. Muons and other particles are produced within a cone-shaped shower, with all particles staying within about 1 degree of the primary particle's path. The muons have a life time of 2.2 microseconds. However, at relativistic speeds, the life time of muon is much longer. Given a minimal 2 GeV muon (rest mass = 0.1 GeV).

2.3 Detectors

Particle detectors are used to detect, track and identify ionising particles. They can measure particle's energy, momentum, spin, charge etc.

Characteristics of detectors

• Acceptance

Acceptance is defined as the ratio of number of particles accepted in a detector to number of particles falling on the detector. In figure 2, we can see a top and bottom plates (paddles) in which muons are falling at zenith angle.

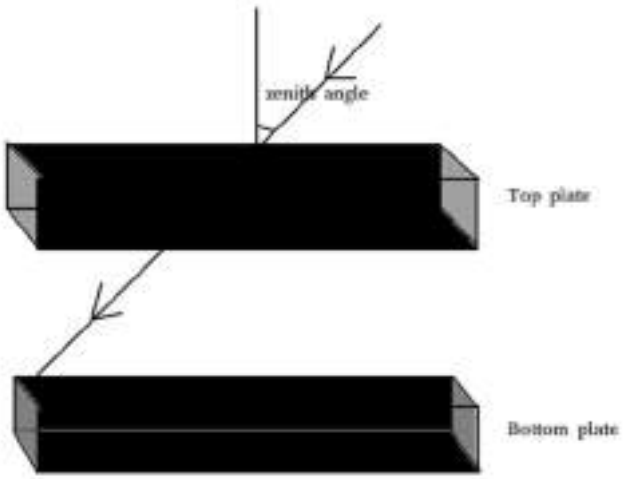

Figure 2: A schematic showing zenith angle

Then, acceptance is the ratio of number of muons striking (top+bottom) plate to the number of muons striking the top plate only.

• Efficiency

Efficiency is defined as the ratio of particles giving the detectable signal with respect to number of particles falling within the geometric acceptance of the detector. It mainly depends on the detector material, it's construction and type of particle.

• **Sensitivity**

The detector sensitivity depends on the following factors:

• the detector mass.

• the detector noise.

• the protection material around the detector.

• **Energy resolution**

Suppose the detector is designed to measure the energy of a particle. Usually, due to fluctuations in the number of excitations and ionizations in the detector material, one observes a Gaussian like peak for a monoenergetic particle beam instead of an ideal delta function peak. The width of this peak determines the capability to distinguish particles with different energies. The energy resolution ΔE is given by the full-width-at-half-maximum (FWHM) of the signal peak. For a Gaussian distribution with standard deviation σ, we have

$$\textbf{FWHM} = 2.35\sigma$$

Energies closer than this resolution cannot be seperated.

• **Response time**

This is the time between the arrival of the radiation and the formation of an output signal. If the signal is formed on a very short time scale with a fast rising flank, a precise moment in time can be marked by the signal. This characteristics is important if timing information is crucial.

- **Dead time**

The process of energy (charge) deposition and the readout of the information takes a finite time in which the detector and its associated electronics is not able to register a subsequent signal. Depending on the type of detector and the rate of particle interactions with the detector material, the issue of dead time can be rather important [3].

2.4 Scintillator Detector

Scintillator material in which light is produced by the passage of particles like electrons, alpha particles etc. They are mainly 2 types, organic scintillators and inorganic scintillators. Generally, organic scintillators are liquid and plastic scintillators. Inorganic scintillators are mainly alkali halides in which sodium iodide is the best. Inorganic scintillators have best light output and linearity, but its response time is very low. Organic scintillators are generally faster, but it gives only less light output. The Z value of constituents and high density of crystals make inorganic scintillators very useful in gamma ray spectroscopy. But, organics are useful for beta spectroscopy and neutron detection. Fluorescence is the process of emission of visible light due to the excitation. There are also other processes that are also produce visible light. They are phosphorescence and delayed fluorescence. But, these two processes take more time for emission. To be a good scintillator, a material should convert as large a fraction as possible of the incident radiation energy to prompt fluorescence, while minimizing the generally undesirable contribution for phosphorescence and delayed fluorescence.

Organic scintillators

The fluorescence process in organic scintillators occur due to transition level structure of a single molecule. It is independent of physical state. For example, anthracene is

observed to fluorescence either as a solid polycrystalline material, as a vapour or as a part of a multicomponent solution. But, it is not similar in inorganic scintillators. For example, sodium iodide which require a regular crystalline lattice for scintillation process. Most of the organic scintillators is based on organic molecules with certain symmetry properties that give rise to π -electron structure. The π -electron structure of such a molecule is given in figure 3.

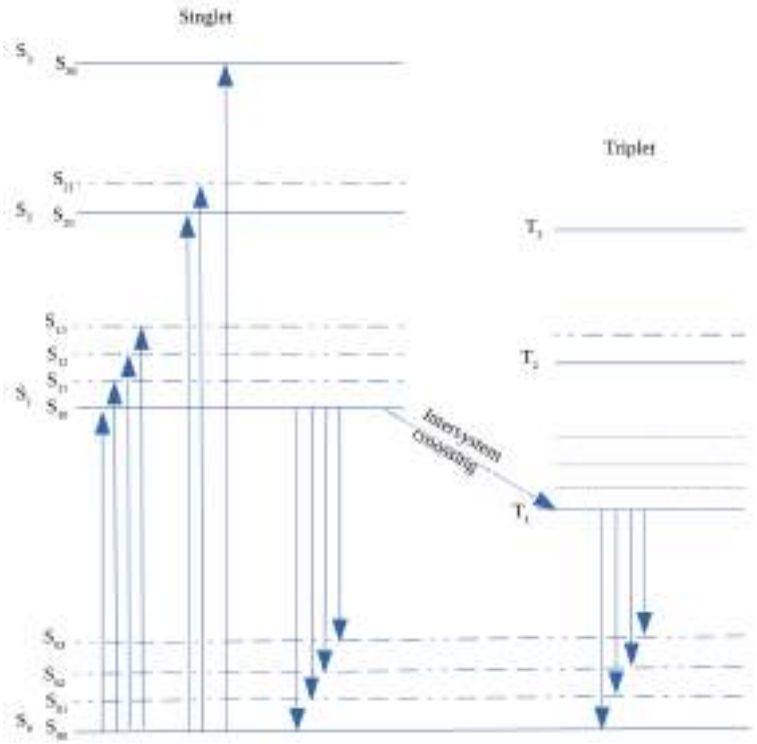

Figure 3: Energy levels of organic molecule with π-electron structure

Energy can be absorbed by exciting the electron configuration into any one of the number of excited states. A series of singlet states (spin 0) are labeled as S_O, S_1, S_2...which is shown in figure. A similar set of triplet states (spin 1) are labeled as T_1, T_2, T_3... In organic scintillators, the energy spacing between S_0 and S_1 is 3 or 4 eV, whereas spacing between higher lying states is usually smaller. Each of these electronic configurations is further subdivided into a series of levels with much finer spacing that corresponds to

various vibrational states of the molecule. Typical spacing of these levels is of the order of 0.15 eV. A second subscript is often added to distinguish these vibrational state of the ground electronic state.

Because the spacing between vibrational states is large compared with average thermal energies, nearly all the molecules at room temperature are in the S_{00} state. By absorbing the kinetic energy of the charged particle, the higher singlet electronic states excited. Then, they de-excited quickly to the S_1 electron state through radiationless internal conversion. Furthermore, any state with excess vibrational energy is not in thermal equilibrium with its neighbours and again quickly loses that vibrational energy. Therefore, the net effect of the excitation process in a simple organic crystal is to produce, after a negligibly short time period, a population of excited molecules in S_{10} state.

The principal scintillation light is emitted in transitions between this S_{10} state and one of the vibrational states of the ground electronic state. These transitions are indicated by downward arrows in Figure 3.

If τ represents the fluorescence decay time for the S_{10} level, then the prompt fluorescence intensity at a time t following excitation should simply be

$$I = I_0 \exp(\frac{-t}{\tau})$$

In most organic scintillators, τ is a few nanoseconds and the prompt scintillation component is relatively fast. The life time of first triplet state T_1 is much longer than that of singlet state S_1. There is a transition called inter system crossing through which some excited singlet states converted into triplet states. The life time of T_1 is very small in the range of nanoseconds and the radiation emitted due to the de-excitation from T_1 to

S_0 is therefore a delayed light emission characterised as phosphorescence. Because, T_1 lies below S_1, the wavelength of the phosphorescence spectrum is longer than that of fluorescence spectrum. While in T_1 state, some molecules excited thermally back to the S_1 state and subsequently decay through fluorescence. This process is origin of delayed fluorescence.

Figure 3 can also be used to explain why organic scintillators can be transparent to their own fluorescence emission. The length of upward arrows corresponds to those photon energies that will be strongly absorbed in the material. Because, all the fluorescence transitions represented by the downward arrows (with the exception of S_{10} - S_{00}) have a lower energy than the minimum required for excitation, there is very little overlap between the optical absorption and emission spectra (often called the Stokes shift) and consequently little self-absorption of the fluorescence.

The scintillation efficiency is defined as the fraction of all the incident particle energy that is converted into visible light. We should prefer scintillator with large efficiency. But, there may present some de-excitation modes which donot involve emission of light and in which excitation is degraded mainly to heat. These process are called quenching. So, in the case of fabrication of scintillators, we must eliminate impurities which may cause quenching [4].

Types of organic scintillators

- **Pure organic crystals**

Only two materials are used as pure organic crystalline scintillators. They are anthracene and stilbene. Anthracene is one of the oldest organic scintillator and its main advantage is that it has high scintillation efficiency. Next one is stilbene, it has low scintillation efficiency but it is used in some cases in which pulse shape discrimination is required to

distinguish between scintillation induced by charged particles and electrons. These two materials are very difficult to obtain in large quantities.

•Liquid organic solutions

This type of scintillators are produced by dissolving organic scintillators in appropriate solvent. The most widely used solvents are toluene, xylene, benzene, phenylcyclohexane, triethylbenzene and decalin. Liquid scintillators are easily loaded with other additives such as wavelength shifters to match the spectral sensitivity range of a particular PMT to increase the neutron detection efficiency of the scintillation counter itself. For many liquids, dissolved oxygen can act as a quenching agent and lead to reduced light output, hence the necessity to seal the solution in an oxygen-free, airtight enclosure. Liquid scintillators are often sold commercially in sealed glass containers and handled as same as solid scintillators. In some cases, large volume detectors with several meters are needed. Then, they are best practical choice from a cost stand point. The counting efficiency is almost 100%.

• Plastic scintillators

If an organic scintillator is dissolved in a suitable solvent and polymerised, it will be equivalent to a solid solution. For example, a solvent consisting of styrene monomer in which an appropriate organic scintillator is dissolved. The styrene is then polymerised to form a solid plastic. They can be easily shaped and fabricated, so they are very useful type of organic scintillators. Plastic scintillators are available in different shapes like rods, cylinders and flat sheets etc. The material is relatively inexpensive, so we can use these if large volumes are needed. Self absorption is one of the problem in plastic scintillators, so attenuation is possible. We must give some attention about attenuation. These plastic scintillators are now using in many high enegy experiments. So, they are

exposed to high energetic radiations. Then, the chance of radiation damage is very high [4].

Response of organic scintillators

• Light output

A small fraction of kinetic energy lost by a charged particle in a scintillator is converted into fluorescent energy. The remainder is dissipated nonradiatively, primarily in the form of lattice vibrations or heat. Scintillation efficiency depends on both particle type and its energy. For organic scintillators like anthracene , stilbene and many liquid and plastic scintillators, the response of electrons is linear for particle energies above 125 KeV. The response to heavy charged particles such as protons or alpha particles is always less for equivalent energies and non linear to higher initial energies.

The response of organic scintillators to charged particles can be described by the relation between $\frac{dL}{dx}$ (the fluorescent energy emitted per unit length) and $\frac{dE}{dx}$ (the specific energy loss for the charged particle). Birks suggested a relation connecting these. In the absence of quenching, the light yield is proportional to energy loss.

$$\frac{dL}{dx} = \mathrm{S}\ \frac{dE}{dx}$$

where S is the normal scintillation efficiency.

• Time response

If it can be assumed that the luminescent states in an organic molecule are formed instantaneously, then the time profile of the light pulse will be very fast. A more detailed model of time dependence of the scintillation yield must take into account two other effects: the finite time required to populate luminescent states and the slower components of the scintillation corresponding to delayed fluorescence and phosphorescence.

Times of approximately half a nanosecond are required to populate the levels from which prompt fluorescence arises. For very fast scintillators, the decay time is 3 or 4 times greater than these levels. Overall shape of the light pulse is given by

$$I = I_0[\exp{(\frac{-t}{\tau})} - \exp{(\frac{-t}{\tau_1})}]$$

where τ_1 is the time constant describing the population of the optical levels and τ is the time constant describing their decay.

The overall light versus time profile is described by the formula given below.

$$\frac{I}{I_0} = f(t)\exp{(\frac{-t}{\tau})}$$

f(t) is the Gaussian function characterised by a standard deviation σ_{ET}. Experimentally, the rise and fall of light output can be characterised by the full width at half maximum (FWHM) of the resulting light versus time profile.

Inorganic scintillators

Inorganic scintillators are usually crystals grown in high temperature furnaces. For example, alkali metal halides, often with a small amount of activator impurity. The most widely used is NaI(Tl) (thallium-doped sodium iodide). It's scintillation light is blue. Other inorganic alkali halide crystals are: CsI(Tl), CsI(Na), CsI(pure), CsF, KI(Tl), LiI(Eu). Some non-alkali crystals include: BaF_2, CaF_2(Eu), ZnS(Ag), GSO, LSO etc [4].

CHAPTER THREE

APPARATUS

3.1 Scintillators

- **Plastic scintillator**

In this experiment, BC-408 Plastic scintillator is used.

Properties of BC-408 Plastic scintillator

- Scintillator base is PolyVinyltoluene.
- Density is 1.023 g/cc.
- Refractive index is 1.58.
- Light output is 64%.
- Rise time is 0.9 ns.
- Decay time is 2.1 ns.
- Pulse width, FWHM is 2.5 ns.
- Light attenuation length is 210 cm [5].

- **Liquid scintillator**

In this experiment, EJ-301 Liquid scintillator is used.

Properties of EJ-301 Liquid scintillator

- Light output is 78%.
- Efficiency is 12000 photons/1MeV.

- Decay time is 3.2 ns.
- Refractive index is 1.505.
- Light attenuation length is 250-300 cm.

- **Dimensions of scintillators**

Table 2: Dimensions of Liquid and Plastic scintillators

Scintillators	Length (cm)	Width (cm)	Height (cm)
Liquid scintillator	100	6	6
Plastic scintillator	100	10	2.5

3.2 Light Guide

It is often impossible to couple a photomultiplier tube directly to one face of the scintillator. Because, the size or shape of the scintillator may not conveniently match the circular photocathode area of commercially available photomultiplier tube. Better light collection efficiency will be achieved by using a transparent solid called light guide which is used to physically couple scintillator to PMT for guiding scintillation light.

Usually, scintillation measurements are to be made in a strong magnetic field. So, PMT must be shielded from the field. So, sometimes it is mounted to a location some distance away from the scintillator. Very thin scintillators should not be mounted directly on the end window to avoid pulse height variations that can araise due to photocathode nonuniformities. A light pipe between the thin scintillator and PMT will spread the light from each scintillation event over the entire photocathode to average out these non uniformities and improve the pulse height resolution.

Light guides are optically transparent solids with relatively high refractive index to minimize the critical angle for total internal reflection. Surfaces are highly polished and are often surrounded by a reflective wrapping to direct back some of the light that escapes at angles less than the critical angle. Lucite is commonly used material that can be transformed into many shapes [4].

3.3 Photomultiplier Tube

Photomultiplier tubes are used to convert the extremely weak light output of a scintillation pulse into a corresponding electrical signal. PMT is used without adding much noise. An outer envelope serves as a pressure boundary to sustain vaccum conditions inside the tube that are required so that low energy electrons can be accelerated efficiently by internal electrical fields. Structure of PMT is shown in figure 4 .

Photomultiplier tube contains a photocathode, several dynodes and an anode. Incident photons strike the photocathode material, which is usually a thin vapour-deposited conducting layer on the inside of the entry window of the device. Electrons are ejected from the surface as a consequence of the photoelectric effect. These electrons are directed by the focusing electrode towards the electron multiplier, where electrons are multiplied by the process of secondary emission. The electron multiplier consists of a number of electrodes called dynodes. Each dynode is held at a more positive potential about 100 Volts than the preceding one. A primary electron leaves the photocathode with the energy of the incoming photon (about 3 eV for blue photons) minus the work function of the photocathode. A small group of primary electrons is created by the arrival of a group of initial photons. The primary electrons move towards the first dynode because, they are accelerated by the electric field. Each of them arrive with 100 eV kinetic energy imparted by the potential difference. Upon striking the first dynode, more

low energy electrons are emitted and these electrons are in turn accelerated towards the second dynode. The geometry of the dynode chain is such that a cascade occurs with an exponentially increasing number of electrons being produced at each stage. The last stage is called the anode. This large number of electrons reaching the anode results in a sharp current pulse that is easily detectable using an oscilloscope.

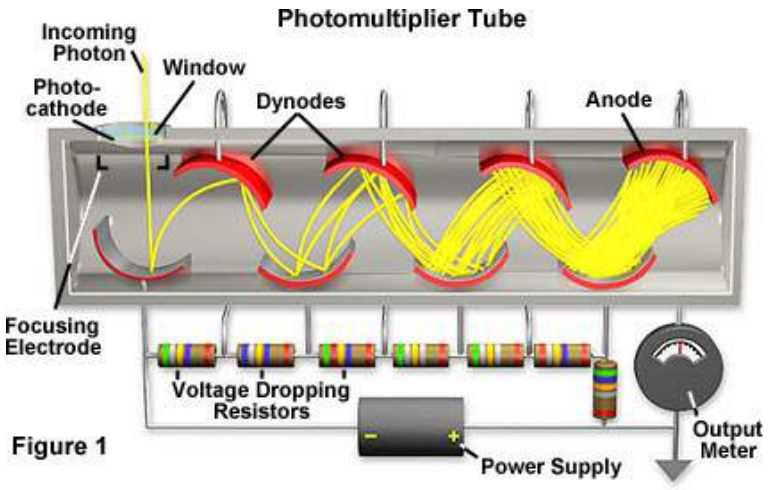

Figure 4: Photomultiplier tube

PMT Characteristics

- **Time characteristics**

Photomultiplier tube is a photodetector that has an exceptionally fast time response. The time response is determined primarily by the transit time required for the photoelectrons emitted from the photocathode to reach the anode after being multiplied as well as the transit time difference between each photoelectron. Accordingly, fast response photomultiplier tubes are designed to have a spherical inner window and carefully engineered electrodes, so that the transit time difference can be minimized.

The time response is mainly determined by the dynode type, but also depends on the supply voltage. Increasing the electric field intensity or supply voltage improves the

electron transit speed and thus shortens the transit time. In general, the time response improves in inverse proportion to the square root of the supply voltage.

•Rise time, Fall time and Electron transit time

Figure 5 represents the rise time, fall time and electron transit time.

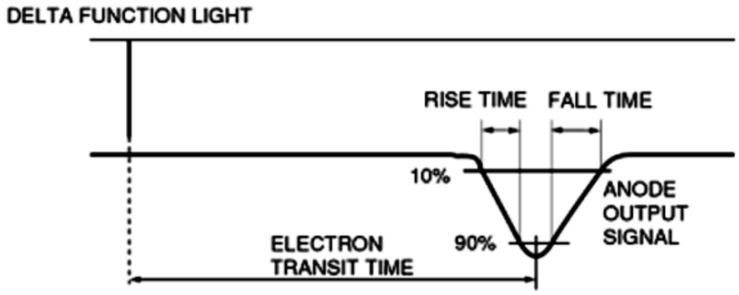

Figure 5: Definition of rise, fall and electron transit time

According to figure 5, the rise time is defined as the time for the output pulse to increase from 10 to 90 percent of the peak pulse height. Conversely, the fall time is defined as the time required to decrease from 90 to 10 percent of the peak output pulse height. In time response measurements where the rise and fall times are critical, the output pulse tends to suffer waveform distortion, causing an erroneous signal. To prevent this problem, proper impedance matching must be provided including the use of a voltage divider circuit with damping resistors.

The transit time is the time interval between the arrival of a light pulse at the photocathode and the appearance of the output pulse. This transit time is a useful parameter in determining the delay time of measurement systems.

In this experiment, we use Hamamatsu R6095 PMT. It is shown in figure 6.

Figure 6: R6095 Photomultiplier tube

Properties of R6095 PMT

- Minimum wavelength is 300 nm.
- Outside diameter is 28 mm.
- Peak wavelength is 420 nm.
- Max.supply voltage is 1500 V.
- Gain is 2x10^6.
- Rise time is 4 ns.
- Photocathode material is Bialkali.
- Window material is Borosilicate.
- Anode current is 0.1 mA [6].

3.4 Voltage Divider

In this experiment, we use E990-07 Voltage divider. It is shown in figure 7.

Figure 7: E990-07 Voltage divider

Properties of E990-07 Voltage divider

- Applicable PMT is 28 mm Head-on type.
- Supply voltage polarity is negative.
- Insulation voltage is 1500 V.
- Supply voltage is 1500 V.
- Voltage divider current is 0.38 mA [7].

3.5 Nuclear Instrument Module (NIM) System

NIM System consists of different modules, each of them having different functions [8]. The NIM bins provide power supply to each modules. The modules are given below.

- **Amplifier**

This is used to amplify the signals from the photomultiplier tube. We can reshape the pulse for our convenience. It is also used to suppress the noise. Here, we are using NIM N568LC Amplifier. It's properties are in the table 3.

Table 3: Properties of NIM N568LC Amplifier

No: of channels	16
Coupling	DC
Shaping	Gaussian Type
Input impedence	50 Ω
Output rise time	25 ns
Equivalent input noise	$<$25 μV

Features of NIM N568LC Amplifier

- 16 Channels.
- Positive or negative inputs accepted on each channel.
- Wide gain range: 0.15 to 480 per channel.

- **Discriminator**

The purpose of the discriminator is to reject pulses smaller than a threshold. If the amplitude of an input pulse is greater than the threshold, the discriminator gives an output pulse. If the amplitude of an input pulse is less than the threshold, the discriminator

does nothing. If the threshold level is very low, we get mostly noise. But, if it is too high, we get nothing. Therefore, correct adjustment of the threshold is one of the most important duty to be performed.

NIM N843 Constant Fraction Discriminator

Table 4: Properties of NIM N843 CFD

Input channels	16 inputs
Max. input voltage	-5 V
Threshold range	-1 mV to -255 mV
Dead time	150 ns to 2 μs

- **Coincidence Units**

Each coincidence unit has two inputs and a switch to choose between AND or OR Gate. There are two pairs of NIM outputs, one fast negative output and one complimentary output.

NIM N455 Coincidence Units

- Max.frequency is 130 MHz
- Input-Output delay is $<$16 ns

N638 Translator

• The Mod. N638 is a standard NIM module housing 16 independent logic level translators.

• The Maximum operating frequency is 300 MHz.

• NIM Inputs have 50 Ω impedance.

3.6 DPO 3054 Oscilloscope

• 500 MHz band width model.

• 2.5 GS/s sample rate on all channels.

• 4 analog channel model.

• Maximum waveform capture rate is greater than 50,000 wfm/s [9].

3.7 VERSA Module Eurocard (VME) System

VME is a Module system like NIM. The module used in our experiment is V862 QDC. It's properties are given below.

• It is charge to digital converter.

• Polarity is negative.

• Maximum input range is 400 pC.

• Full 12-bit resolution.

• 32 channel individual Gate QDC.

3.8 RG 174 A/U Coaxial Cable

RG 174 A/U type Coaxial cable is used in the experiment [10]. It is shown in figure 8.

Figure 8: RG 174 A/U Coaxial cable

Properties of RG 174 A/U Coaxial cable

- Characteristic impedence is 50 Ω.
- Time delay is 5.05 ns/m.
- Maximum voltage is 2000 V.
- Maximum frequency is 1 GHz.

CHAPTER FOUR

FABRICATION OF THE DETECTOR

Components required for the experiment shown in figure 9.

Figure 9: Different components used in the experiment

In figure 9, we can see the components like plastic scintillator, photomultiplier tube, light guide, voltage divider, tyvek paper, tedler paper etc. First, we fixed the plastic scintillator with light guide properly using an optical cement. Here, we used EJ-500 Optical cement. It includes an optical cement resin and optical cement hardner. For proper optical bonding between plastic scintillator and light guide, we mixed these two properly. We spent 3 hours to set the cement and then applied it on the faces of both

plastic scintillator and light guide. Approximately, it took 1 day for harden properly.

Figure 10: Fixing of plastic scintillator and light guide using optical cement

Properties of EJ-500 Optical cement

Table 5: Properties of Optical cement

Mixed viscosity (cps)	800
Dielectric strength (Volts/mil)	420
Specific gravity	1.17
Service temperature (^oC)	-65 to 105 [11]

In figure 11, the fixed plastic scintillator and light guide is placed over a reflecting paper called tyvek paper. It is used for avoiding optical loss.

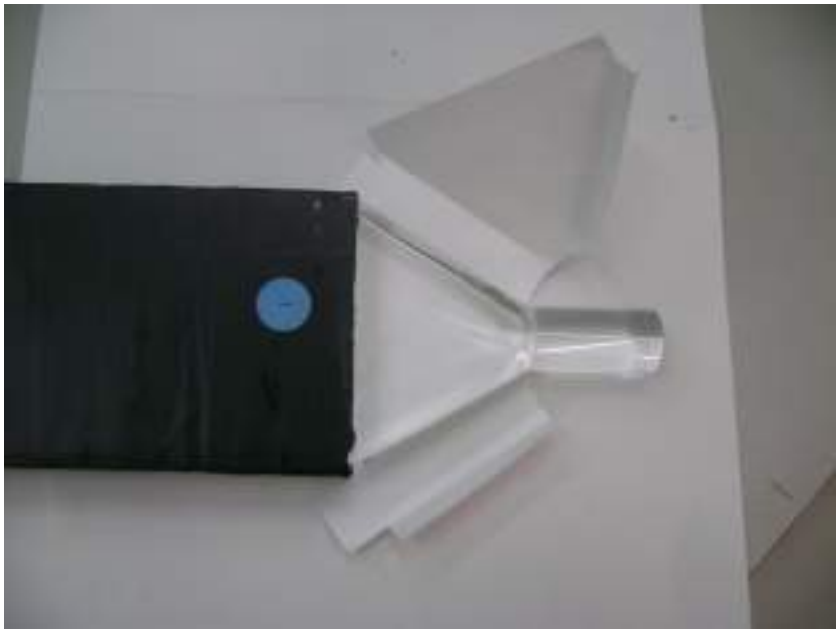

Figure 11: plastic scintillator and light guide with a tyvek paper

We covered the light guide with a tyvek paper properly shown in figure 12.

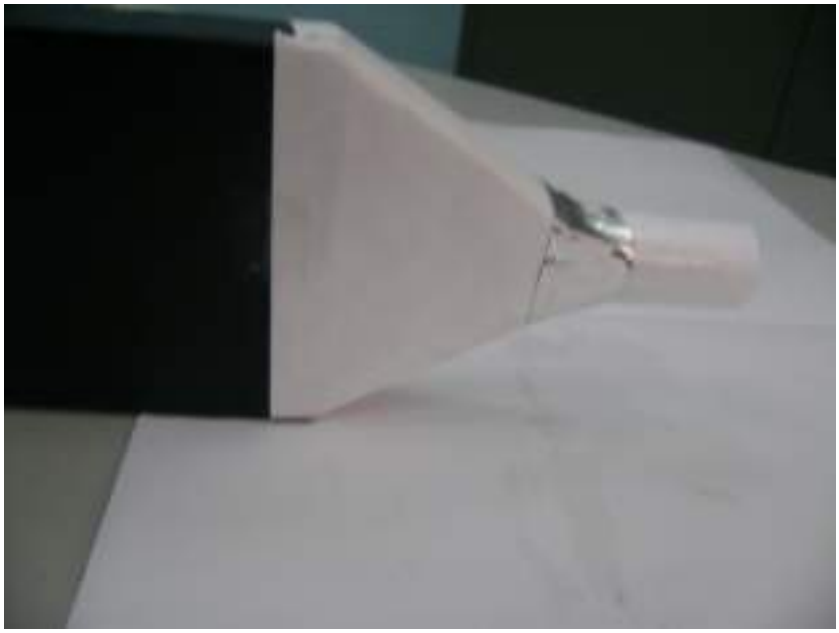

Figure 12: Proper covering with a tyvek paper

We covered the light guide using a tedler paper over the tyvek paper. In figure 13, we can see a metallic coupler.

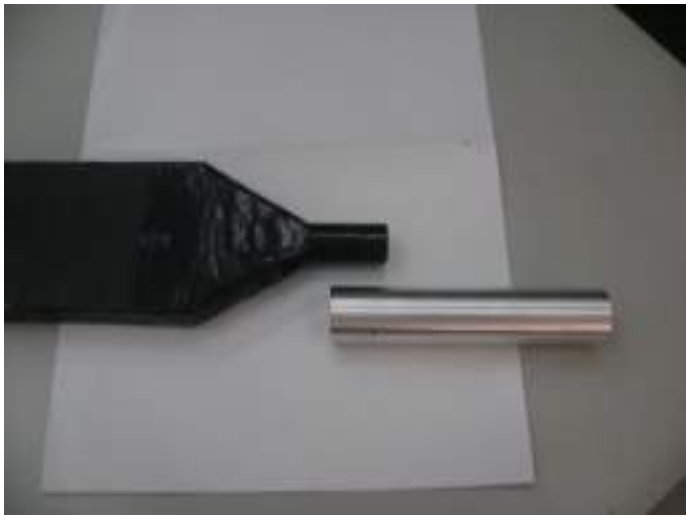

Figure 13: metallic coupler with plastic scintillator setup

We fixed the PMT to the light guide using an optical cement. A metallic coupler is used to cover the PMT. Metallic coupler is used only for the mechanical support. A voltage divider is fitted behind PMT which leads to oscilloscope.

Figure 14: Proper fitting of PMT and voltage divider

CHAPTER FIVE

EXPERIMENTAL PROCEDURE

Our principle aim to detect atmospheric muons from plastic scintillator and measure the muon particle flux. While connecting the pulse to oscilloscope, we got numerous pulses like gamma rays, muons and other noises. It was very difficult to identify muon particles. So, coincidence was essential. Next, we took 3 liquid scintillators. Pulses from each of the three scintillators were given to NIM Modules through coaxial cables. We connected the 3 pulses to Constant Fraction Discriminator. Then, we got logic pulses. The outputs from this is given to input of the coincidence unit. Connected the output of coincidence unit into oscilloscope. So, we got 2 pulses. One is from the PMT of our plastic scintillator and the other is from the coincidence unit. The pulses are shown in figures 15 and 16. As already mentioned above that many particles are coming from our plastic scintillator along with muon particles. But, we need only muon particles. So, to avoid all other particles, coincidence is essential.

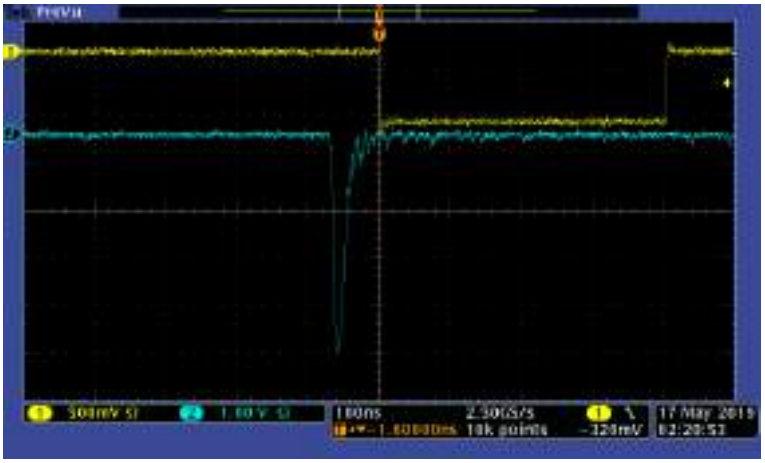

Figure 15: Picture of pulses taken from the oscilloscope

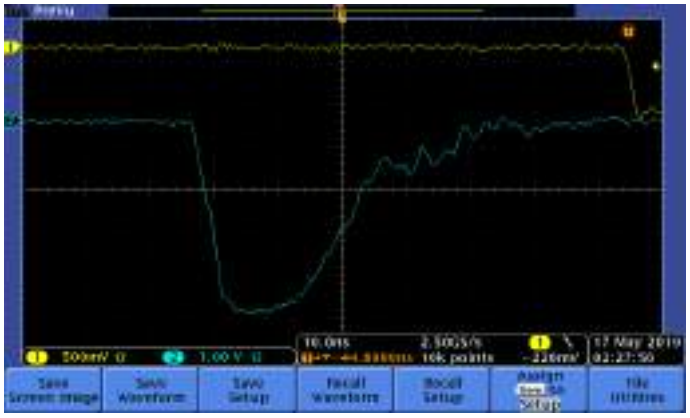

Figure 16: Picture of pulses taken from the oscilloscope

Analog pulse (blue coloured) is from the PMT of our detector. Digital pulse (yellow coloured) is from coincidence unit. Analog pulse is only from atmospheric muons. From figure 15, there occured a time delay of 100 ns between the 2 pulses. For efficiency measurements, we have to avoid this delay. To fix this, we used coaxial cable. The experimental setup is shown in figure 17.

Figure 17: Experimental setup

In the experimental setup, we can see plastic scintillator and different liquid scintillators.

CHAPTER 6

RESULTS AND DISCUSSION

6.1 Rise time

We measured the rise time of both liquid and plastic scintillators by analysing the pulses which have seen in the oscilloscope. The measurements are given in the table 6.

Table 6: Rise time of liquid and plastic scintillators

Liquid scintillator (ns)	Plastic scintillator (ns)
10	9
8.4	17.8
7.2	11.6
10.4	10.8
8.8	11.2
8	17.2
11.2	12.4
8	11.6
7.6	10
8	11.6
10.8	13.2
9.6	14.4
10.4	8.8
11.6	12.8
13.6	14.4

Then, we calculated the error in rise time using the equation,

$$\text{Error} = \sqrt{\frac{\Sigma(x_i - x_m)^2}{N}}$$

Here, x_m and x_i are the average and measured value of rise time respectively and N is the total number of measurements taken.

Average rise time of liquid scintillator = 9.57 $\pm$ 1.73 ns

Average rise time of plastic scintillator = 12.45 $\pm$ 2.54 ns

6.2 Efficiency

We used 4 paddles which are shown in figure 18. In figure, we can see one plastic scintillator and 3 liquid scintillators.

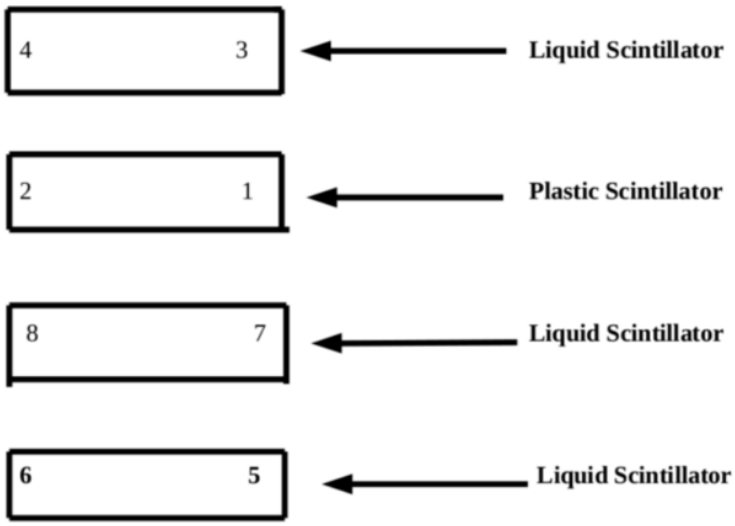

Figure 18: Schematic representation of the paddles

To find the efficiency of the plastic scintillator, we applied voltages in 3, 7, 6 and 1.

The pulses from 3, 7 and 6 are splitted into 2. One is given to CFD and the other is given to QDC with a delay of 100 ns. Outputs from the CFD connected to the coincidence unit. Then, we put the triggered gate pulse from 3, 7 and 6 to QDC. We started the data acquisition. From computer, we got the number of counts (events) and the corresponding time in seconds. So, it was easy to measure the number of events occured in one second.

Applied voltage = 1500 V

Number of counts (events) (N2) = 880

Time elapsed (t2) = 2314 s

Counts / Second (N2S) = 0.376 s^{-1}

Paddle 1.1

Next, we gave the coincidence pulse of 3, 7, 6 and 1 into QDC. The overall connection diagram is shown in figure 19.

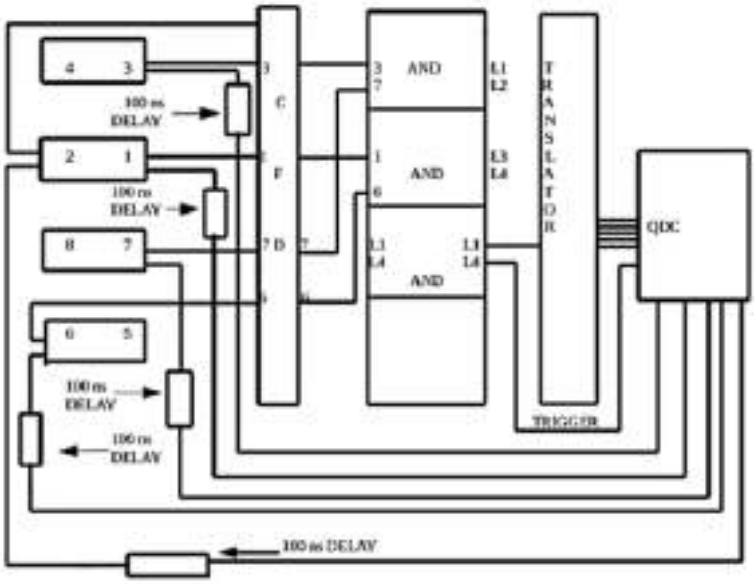

Figure 19: Coincidence of 3, 7, 6 and 1

From data acquisition, we measured the number of events occured in one second (N1S). We applied different voltages in 1 and measured the corresponding counts per second. The measurements are given in the table 7.

Table 7: Event rate in the coincidence of 3, 7, 6 and 1 occured in paddle 1.1

Voltage applied in 1	Time elapsed (t1)	Number of counts (N1)	Counts/second (N1S) (s^{-1})
1100 V	1041 s	35	0.034
1150 V	1148 s	136	0.118
1200 V	1450 s	341	0.235
1250 V	1125 s	370	0.329
1350 V	1043 s	364	0.349
1400 V	1155 s	424	0.367
1450 V	1177 s	389	0.331
1500 V	1214 s	422	0.348
1550 V	1259 s	453	0.36
1600 V	1915 s	681	0.356

From these data, we can calculate the efficiency of the paddle.

$$\text{Efficiency} = \text{N1S} / \text{N2S}$$

N1S is the number of counts per second in the coincidence of 3, 7, 6, 1. N2S is the number of counts per second in the coincidence of 3, 7, 6.

From the equation, we calculated the efficiency for each of the voltage. Then, we plot the graph between efficiency and voltage and put error bars on the graph. We calculated the error using equation given below.

$$\text{Error in efficiency} = \sqrt{e1 \times e1 + e2 \times e2}$$

Here, e1 = $\frac{\sqrt{N1}}{N1}$ and e2 = $\frac{\sqrt{N2}}{N2}$.

N1 = Number of events occured in the coincidence of 3, 7, 6 and 1.
N2 = Number of events occured in the coincidence of 3, 7 and 6.

Then, we plot the efficiency curve. The curve is shown in figure 20.

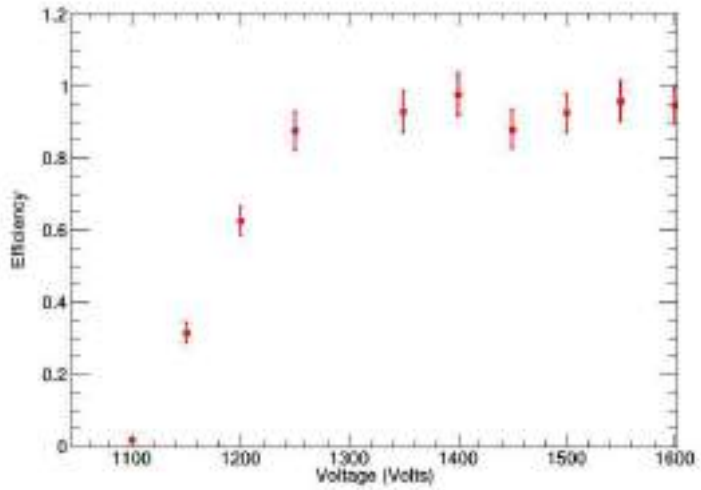

Figure 20: Efficiency curve of paddle 1.1

The operating voltage is taken as 1400 V.

Paddle 1.2

Next, we gave the coincidence pulse of 3, 7, 6 and 2 into QDC. The overall connection diagram is shown in figure 21.

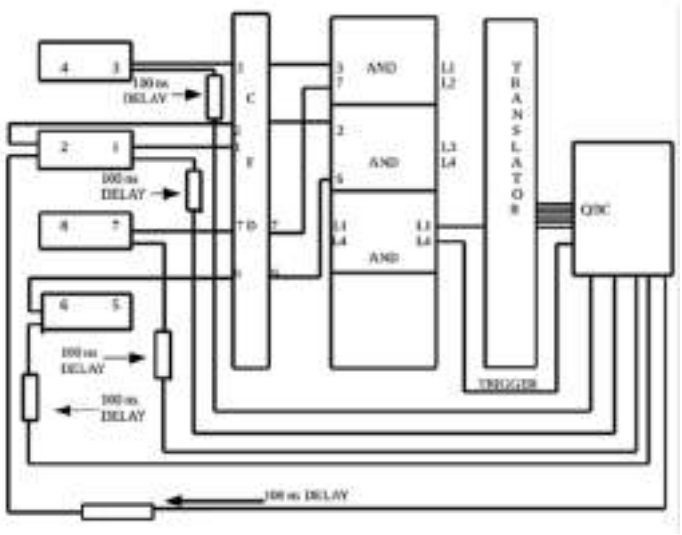

Figure 21: Coincidence of 3, 7, 6 and 2

From data acquisition, we measured the number of events occured in one second (N1S). We applied different voltages in 2 and measured the corresponding counts per second. The measurements are given in the table 8.

Table 8: Event rate in the coincidence of 3, 7, 6 and 2 occured in the paddle 1.2

Voltage applied in 2	Time elapsed (t1)	Number of counts (N1)	Counts/second (N1S) (s^{-1})
850 V	19 s	1208	0.02
900 V	1211 s	60	0.05
950 V	1323 s	266	0.20
980 V	1585 s	512	0.32
1000 V	1193 s	392	0.33
1100 V	2283 s	753	0.33
1150 V	1162 s	366	0.32
1200 V	1017 s	326	0.32
1250 V	529 s	175	0.33

From these data, we plot the corresponding efficiency curve with error bars which is given in figure 22.

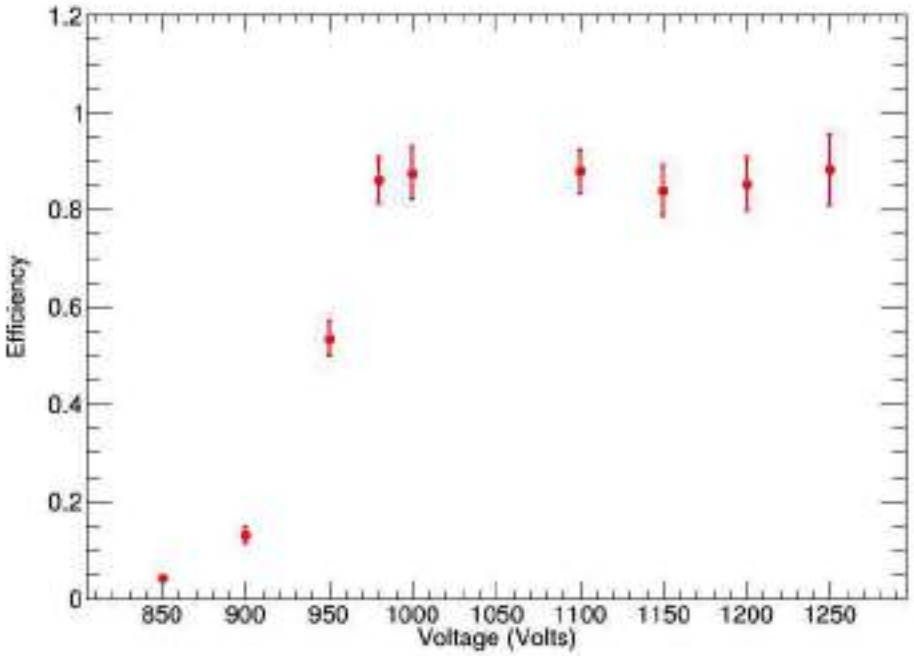

Figure 22: Efficiency curve of paddle 1.2

The operating voltage is taken as 1100 V.

Paddle 2.1

We replaced the plastic scintillator with a new one. We decided to find the efficiency of the new one. The connection diagram is same which is given in figure 19. The only thing we have done is the replacement of scintillator. We applied voltages in 2, 3, 6, 7. Then, we applied different voltages in 1 and measured the corresponding number of counts in one second which is given in the table 9.

Table 9: Event rate in the coincidence of 3, 7, 6 and 1 occured in the paddle 2.1

Voltage applied in 1	Time elapsed (t1)	Number of counts (N1)	Counts/second (N1S) (s^{-1})
1200 V	730 s	248	0.34
1250 V	709 s	244	0.34
1350 V	2053 s	780	0.38
1400 V	3525 s	1200	0.34
1450 V	1811 s	638	0.35
1500 V	1622 s	535	0.33
1550 V	730 s	250	0.34

From these data, we calculated the error in efficiency and plotted the corresponding efficiency curve which is given in figure 23.

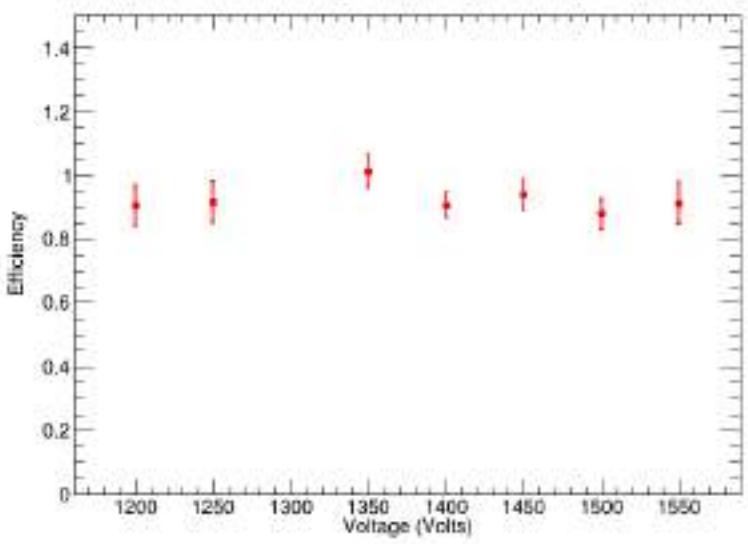

Figure 23: Efficiency curve of paddle 2.1

Paddle 2.2

We changed the connection diagram which is similar to figure 21. We applied different voltages in 2 and measured the corresponding counts per second from data acquisition. The measurements are given in the table 10.

Table 10: Event rate in the coincidence of 3, 7, 6 and 2 occured in the paddle 2.2

Voltage applied in 2	Time elapsed (t1)	Number of counts (N1)	Counts/second (N1S) (s^{-1})
1200 V	991 s	298	0.30
1300 V	678 s	221	0.33
1350 V	811 s	272	0.34
1400 V	707 s	246	0.35

After getting efficiency, we plotted the efficiency curve which is given in figure 24.

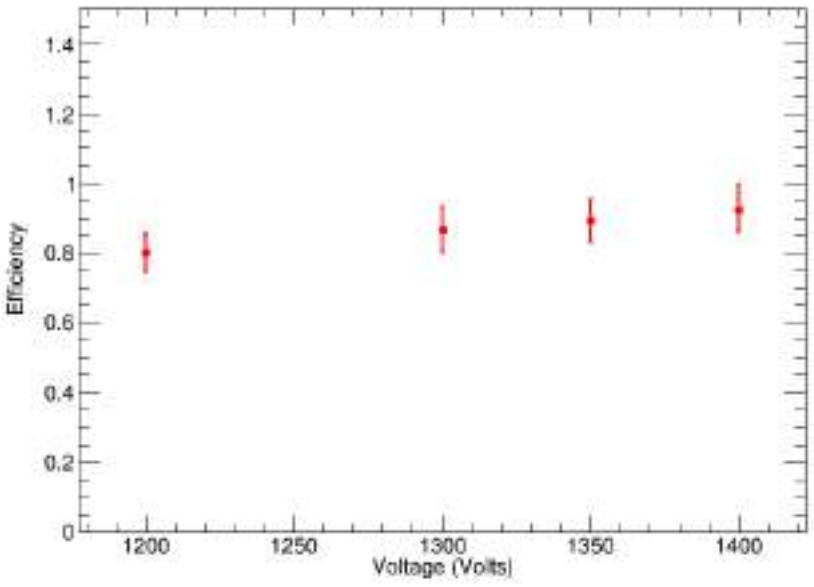

Figure 24: Efficiency curve of paddle 2.2

6.3 Zenith angle distributions

To plot zenith angle distributions, we used 3 plastic scintillators and one liquid scintillator arranged in proper distance. The arrangement is shown in figure 25.

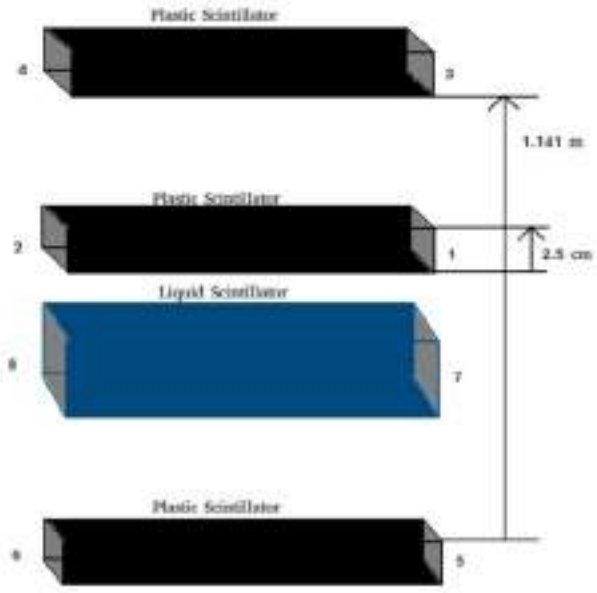

Figure 25: Setup of the paddles

We applied different voltages in the paddles. Applied voltages are given in the table 11.

Table 11: Applied voltages in different paddles

Output	Paddle	Voltage (V)
1	Plastic 3.1	1350
2	Plastic 3.2	1400
3	Plastic 1.1	1400
4	Plastic 1.2	1400
5	Plastic 2.1	not used
6	Plastic 2.2	1400
7	Liquid	1500
8	Liquid	1550

We chose the trigger from 2 & 4 & 6 and 1 & 4 & 6. We took data for different distances, durations and thresholds. Then, we plotted zenith angle distributions which are shown in the figures 26, 27, 28, 29 and 30.

• Zenith angle distribution on top and bottom paddles for seperation distance 1.14 m (Run time = 1651.6 s) is given in the figure 26.

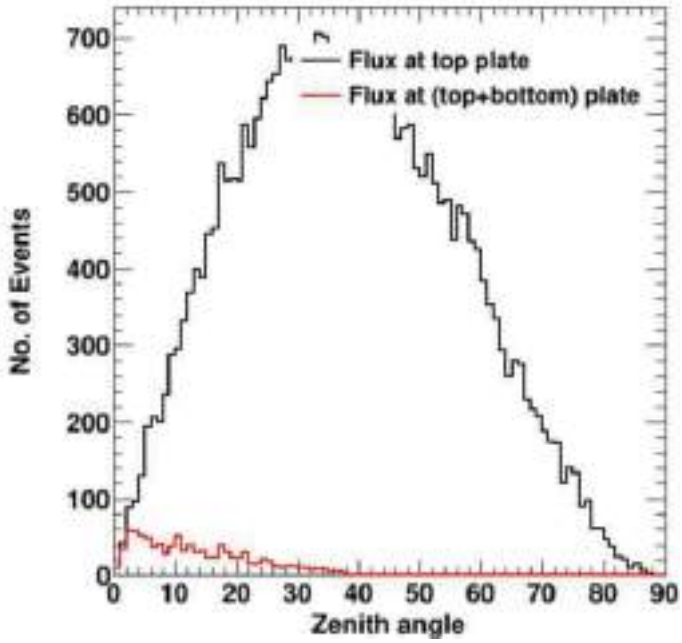

Figure 26: Variation of total number of muons on top and bottom paddles with zenith angle for seperation distance 1.14 m.

• Zenith angle distribution on top and bottom paddles for seperation distance 1.14 m (Run time = 1389 s) is given in the figure 27.

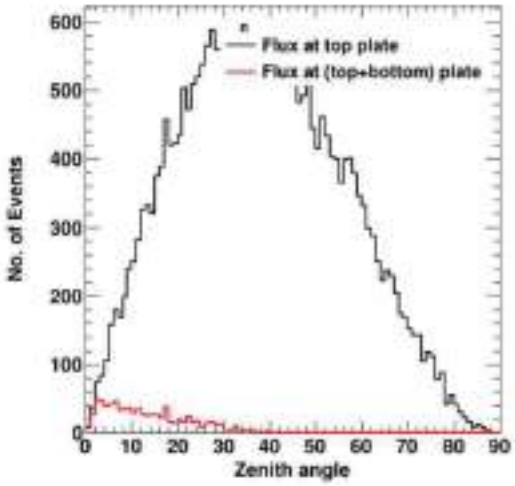

Figure 27: Variation of total number of muons on top and bottom paddles with zenith angle for seperation distance 1.14 m.

• Zenith angle distribution on top and bottom paddles for seperation distance 0.685 m (Run time = 1391 s) is given in the figure 28.

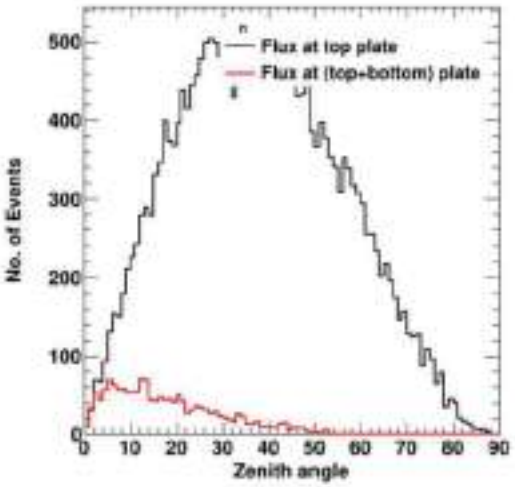

Figure 28: Variation of total number of muons on top and bottom paddles with zenith angle for seperation distance 0.685 m.

• Zenith angle distribution on top and bottom paddles for seperation distance 0.685 m (Run time = 1092 s) is given in the figure 29.

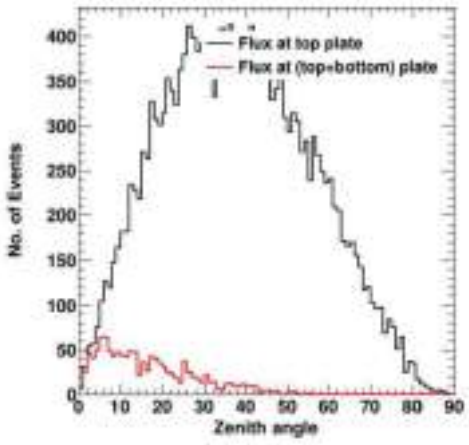

Figure 29: Variation of total number of muons on top and bottom paddles with zenith angle for seperation distance 0.685 m.

• Zenith angle distribution on top and bottom paddles for seperation distance 0.685 m (Run time = 1359 s) is given in the figure 30.

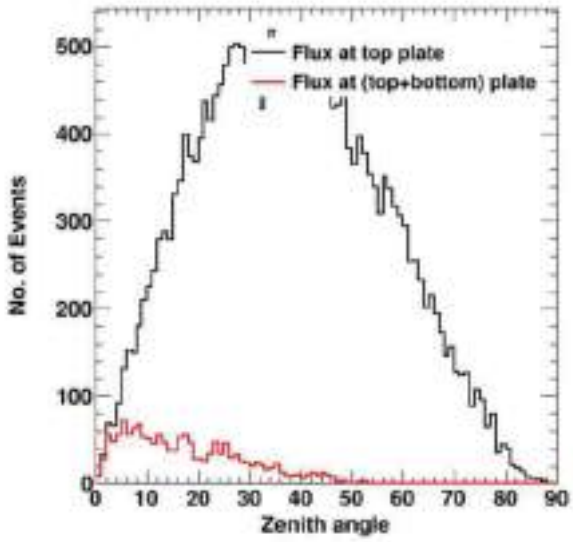

Figure 30: Variation of total number of muons on top and bottom paddles with zenith angle for seperation distance 0.685 m.

6.4 Muon flux measurement

Atmospheric muon flux is defined as the number of counts in one second per unit area per unit acceptance per unit solid angle. Acceptance is obtained from Monte Carlo simulations using input function $\cos^2\theta\sin\theta$.

Area of the detector = 0.1 $\times$ 1 m^2 = 0.1 m^2.

Solid angle = $2\pi/3$.

Then, we measured the flux with errors in all the cases using the equation,

$$\text{Error } e_i = \frac{\sqrt{N_i}}{acceptance \times area \times solidangle}$$

Here, N_i is the number of counts taken. Then, we calculated the statistical error.

$$\text{Statistical error} = \frac{\sqrt{\Sigma e_i^2}}{N}$$

Here, N is the number of measurements taken. We took 5 measurements for our experiment. In addition to statistical error, there will be systematic error also.

$$\text{Systematic error} = \sqrt{\frac{\Sigma(x_i - x_m)^2}{N}}$$

Here, x_m is the mean value of flux. We got the value of x_m is 91.15. In the equation, x_i is the measured value of flux in each trigger. Details of muon flux measurements are given in the table 12.

Table 12: Atmospheric muon flux measurement

Trigger	Distance (m)	Acceptance	Counts	Time (s)	Counts/s (s^{-1})	Flux = $\frac{Counts/s}{Acceptance \times Area \times SolidAngle}$
2&4&6	1.14	0.0289	976	1651.6	0.591	97.66 $\pm$ 3.13
1&4&6	1.14	0.0289	824	1389	0.593	97.99 $\pm$ 3.42
1&4&6	0.685	0.0624	1556	1391	1.12	85.71 $\pm$ 2.17
2&4&6	0.685	0.0624	1237	1092	1.133	86.71 $\pm$ 2.47
2&4&6	0.685	0.0624	1558	1359	1.146	87.7 $\pm$ 2.22

$$\text{Mean flux} = 91.15 \pm 1.22 \pm 5.48\ (\text{m}^{-2}s^{-1}sr^{-1}).$$

Here, 1.22 and 5.48 are the values of statistical and systematic error.

CHAPTER SEVEN

CONCLUSIONS AND FUTURE SCOPE

While doing experiment, we fabricated 3 detector setup using plastic scintillator of dimension 100 cm $\times$ 10 cm $\times$ 2.5 cm, light guide, tyvek paper, tedler paper, PMT and voltage divider. Using light guide, we made a coupling between scintillator bars and PMT. Proper covering of light guide with tyvek and tedler paper prevented optical leak. After applying appropriate voltages to PMT, we analysed pulses and measured the rise time of both plastic and liquid scintillators with errors. We observed that rise time of our plastic scintillator is greater than that of liquid scintillator. The rise time of both plastic and liquid scintillators are 12.45 $\pm$ 2.54 and 9.57 $\pm$ 1.73 ns. Then, we measured the efficiency of each paddle and plotted the efficiency curves. The paddle 1.1 has maximum efficiency of 97%. From efficiency curve, we decided it's operating voltage as 1400 V. In this voltage, it shows maximum efficiency. The efficiencies of the paddles 1.2, 2.1 and 2.2 are 87%, 94% and 93% with operating voltages 1100 V, 1450 V and 1400 V respectively. From zenith angle distributions, we understood that muon flux is large in top plate. Very few atmospheric muons are detected by both top and bottom plate. The probability of acceptance in the case of bottom plate is small. Our main objective of this experiment is to find the muon flux reaching the earth. We calculated the flux with statistical and systematic errors. The value of muon flux is 91.15 $\pm$ 1.22 $\pm$ 5.48 $\mathrm{m}^{-2}s^{-1}sr^{-1}$.

References

[1] *Cosmic Rays* - R A Mewaldt (California Institute Of Technology) published in Macmillan Encyclopedia of Physics (1996).

[2] *Cosmic Ray Experiment* - Steve Kliewer (Endeavour Academy).

[3] *Basic detector concepts* - retrieved from https://www.ippp.dur.ac.uk/ krauss/Lectures/QuarksLeptons/Basics/Det_1.html.

[4] *Radiation Detection and Measurement* - GLENN F.KNOLL

[5] *Retrieved from - https://www.crystals.saint-gobain.com/sites/.../bc400-404-408-412-416-data-sheet.pdf.*

[6] *R6095 Data Sheet* - Hamamatsu Photonics.

[7] *D-Type Socket Assemblies* - retrieved from https://www.hamamatsu.com/resources/pdf/etd/PMT.pdf.

[8] CAEN Product Catalog

[9] Tektronix DPO 3000 Series Digital Phosphor Oscilloscope User Manual.

[10] *Retrieved from - https://www.koax24.de/en//coaxial-cable/koaxial kabel-50..../rg 174-au.html.*

[11] *Retrieved from - https://eljentechnology.com/image/products/data sheets/EJ-500.pdf.*